



INSTITUTE FOR DEFENSE ANALYSES

**Imaging with Amplitude and
Intensity Interferometers**

Frank S. Rotondo

June 2004

Approved for public release;
distribution unlimited.

IDA Document D-2999

Log: H 04-001034
Copy

This work was conducted under contract DASW01 04 C 0003, IDA Central Research Project Task CRP-2084. The publication of this IDA document does not indicate endorsement by the Department of Defense, nor should the contents be construed as reflecting the official position of that Agency.

© 2004 Institute for Defense Analyses, 4850 Mark Center Drive, Alexandria, Virginia 22311-1882 • (703) 845-2000.

This material may be reproduced by or for the U.S. Government.

INSTITUTE FOR DEFENSE ANALYSES

IDA Document D-2999

**Imaging with Amplitude and
Intensity Interferometers**

Frank S. Rotondo

PREFACE

This work was prepared under IDA Central Research Project titled “Imaging Interferometry.” The author acknowledges Roger Sullivan, James Ralston, Bertrand Barrois for their substantive comments.

CONTENTS

I.	INTRODUCTION	I-1
II.	AMPLITUDE INTERFEROMETRY	II-1
	A. Response to a Distant Point Source	II-1
	B. Response to an Extended Source	II-4
	C. The Amplitude Interferometer as an Imaging Device	II-5
	D. Visibility and Source Morphology.....	II-7
	1. Point Source	II-7
	2. Binary System of Point Sources.....	II-7
	3. Flat Source Distribution	II-8
	4. Circular Source Distribution	II-9
III.	INTENSITY INTERFEROMETRY	III-1
	A. Model for an Incoherent (Thermal) Source	III-1
	B. Derivation of the HBT Effect	III-3
	C. Advantages and Limitations of the HBT Effect	III-7
	D. Extension of HBT	III-8
IV.	Summary	IV-1
	REFERENCES	R-1

FIGURES

1. Schematic Diagram of an Interferometer..... II-2
2. Response of an Amplitude Interferometer to an Extended Source..... II-6
3. Visibility versus Baseline for (1) a Binary System of Point Sources Separated by Angle α , (2) a Flat Source that Subtends an Angle α , and (3) a Circular Source (Disk) that Subtends an Angle α II-8
4. Geometry for a Circular (Disk-Shaped) Source that Subtends an Angle α II-10
5. Elements of an Intensity Interferometer III-2
6. Schematic Diagram of an Intensity Interferometer Viewing a Source III-3
7. Path Length Difference for Radiation Arriving at Detectors a and b III-6

I. INTRODUCTION

Interferometers measure the correlation of radiation fields that have taken different paths through space. Astronomers have widely used interferometers because the angular resolution of the device goes as λ/B , where λ is the wavelength of the radiation and B is the separation, or baseline, of the detector elements in the interferometer. Thus, for a given wavelength it is possible to improve an interferometer's resolution by increasing its baseline, and though there are technical difficulties associated with this, it is nonetheless an effective means of improving resolution as opposed to increasing the diameter of a single-aperture imaging system.

Interferometers used by astronomers come in two broad classes: amplitude interferometers and intensity interferometers. Each can, within its own set of limitations, be used to image remote objects. This report, which was funded as a Central Research Project by the Science and Technology Division of the Institute for Defense Analyses, gives an introduction to the subjects of amplitude and intensity interferometry.

Obviously, there are many references that discuss interferometry. I have drawn from a few to compile this report. Born and Wolf's classic text on optics is a first-rate, broad reference to the field [1]. Boden's chapter in the 1999 Michelson Summer School course notes is an excellent introduction to amplitude interferometry [2]. The original article on the subject of intensity interferometry by Hanbury Brown and Twiss provides unique intuition into the subject, and it has historical significance [3]. Thompson, Moran, and Swenson's text on radio interferometry in astronomy is a single, comprehensive reference on the various interferometric techniques used by astronomers [4].

The response of an amplitude interferometer and its application as an imaging device is given in Section II of this report. Section III presents the response of the intensity interferometer and shows how, as an imaging tool, it is limited to measuring source sizes in a model-dependent manner. Extensions to intensity interferometry are also introduced in the chapter, in particular the methods of Gamo [5] and Mehta [6] and the experiment by Beard [7], all of which superimpose a known reference beam on a source, enabling intensity interferometers to fully image a source distribution.

The interferometric imaging techniques covered in this document have the functionality of a lens and focal plane array when imaging distant objects. They further have the flexibility to improve resolution by expanding the baseline of the interferometer beyond the size scales of traditional lens/focal plane array systems. Interferometers consequently have great potential when high-resolution images of distant objects are desired.

II. AMPLITUDE INTERFEROMETRY

Consider the interferometer pictured in Figure 1. The radiation field from a source falls on two apertures, A_1 and A_2 , separated by baseline B . The fields that enter A_1 and A_2 are combined after passing through the two arms of the interferometer, which contain delays d_1 and d_2 . The detected intensity is the square of the sum of the field amplitudes at the point that they are combined. The relative phase of the fields at that point will determine if the field amplitudes constructively or destructively interfere.

Such an interferometer could be constructed with a pair of linear detectors* followed by cables of lengths d_1 and d_2 , which are fed into circuitry whose power output is the square of the sum of the signal amplitudes at the circuit's input. The device could also be a Young's double-slit interferometer where the two apertures are cut in an aperture screen and the field combination is seen on an image screen positioned behind the apertures. In this case, the relative delays d_1 and d_2 would be represented by the position viewed on the image screen along the line parallel to the apertures' baseline. Whatever its manifestation, this class of device is referred to as an *amplitude interferometer*, because the detected intensity results from the square of the sum of the field amplitudes detected by the interferometer.

A. RESPONSE TO A DISTANT POINT SOURCE

Consider a quasi-monochromatic point source with wave number $k = 2\pi/\lambda$ (where λ is the wavelength of the source) at an angle θ from the normal to the baseline of the device. Assume that θ is small ($\sin \theta \approx \theta$), that the source is distant so that its wave-front is a plane wave at the interferometer, and that the apertures and responses in each interferometer arm are equal. The amplitude of the combined signal, a_{net} , is determined by the relative phase of the signals in the spectrometer arms, a_1 and a_2 (common phase factors can be absorbed into an overall constant and are of no consequence):

$$a_{net} = a_1 + a_2 \sim \cos(kB\theta + kd_1 - \omega t) + \cos(kd_2 - \omega t) \quad .$$

* A linear detector is one whose voltage output is proportional to the amplitude of the input field.

In an amplitude interferometer, we will observe the *time-averaged* power, I , of the combined field, where the time average is over a period T that is much larger than the period of the radiation. Note that this is not the instantaneous power, which, for frequencies above about 1 GHz, is not practical to observe. Since I is proportional to the square of the combined amplitude, we have

$$\begin{aligned}
 I &\propto \frac{1}{T} \int_{-T/2}^{T/2} a_{net}^2 dt \\
 &= \frac{1}{T} \int_{-T/2}^{T/2} [\cos(kB\theta + kd_1 - \omega t) + \cos(kd_2 - \omega t)]^2 dt \\
 &= \frac{1}{T} \int_{-T/2}^{T/2} [\cos^2(kB\theta + kd_1 - \omega t) + \cos^2(kd_2 - \omega t) + 2 \cos(kB\theta + kd_1 - \omega t) \cos(kd_2 - \omega t)] dt
 \end{aligned}$$

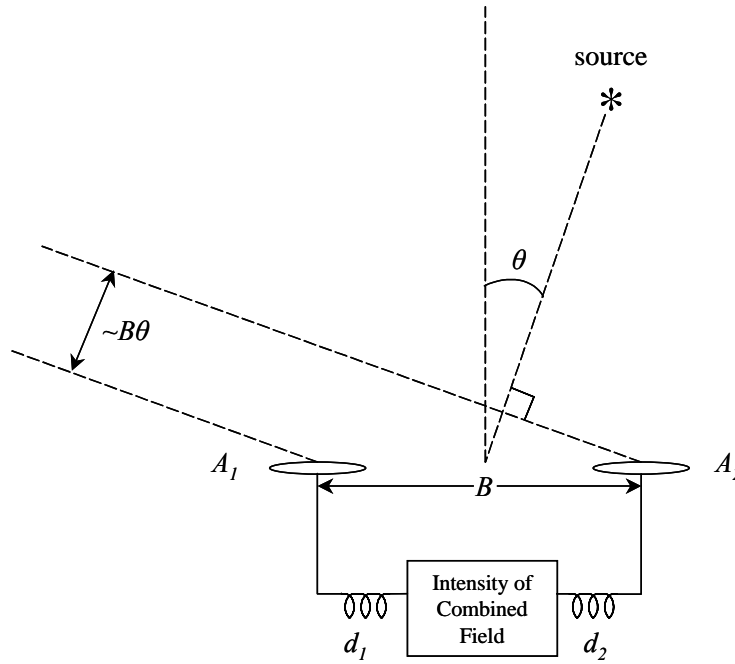


Figure 1. Schematic Diagram of an Interferometer

Using the identities $\cos x \cos y = \frac{1}{2}[\cos(x+y) + \cos(x-y)]$ and $\cos^2 x = \frac{1}{2}[1 + \cos 2x]$, we get

$$\begin{aligned}
 I &\propto \frac{1}{T} \int_{-T/2}^{T/2} [1 + \frac{1}{2} \cos(2kB\theta + 2kd_1 - 2\omega t) + \frac{1}{2} \cos(2kd_2 - 2\omega t) + \\
 &\quad \cos(kB\theta + k[d_1 + d_2] - 2\omega t) + \cos(kB\theta + k[d_1 - d_2])] dt
 \end{aligned}$$

The second, third, and fourth terms, which are cosines whose angles contain an ωt term, will integrate to zero, leaving

$$I \propto \frac{1}{T} \int_{-T/2}^{T/2} [1 + \cos(kB\theta + k[d_1 - d_2])] dt$$

or simply

$$I \propto 1 + \cos(kB\theta + k[d_1 - d_2]).$$

If the flux, or energy per time per area, at both apertures is F , and if the apertures each have equal area A , then the time-averaged power from the point source is

$$I = 2AF[1 + \cos(kB\theta + \delta)] \quad (1)$$

where $\delta = k(d_1 - d_2)$.

Equation 1 generates a fringe pattern that oscillates between 0 and $4AF$, where AF is the power collected by one of the apertures. We could adjust the relative delay δ to a value $-kB\theta \pm n2\pi$, where $n = 0, 1, 2, \dots$, to obtain the fringe at its maximum, representing total constructive interference. Total destructive interference is obtained when $\delta = -kB\theta \pm n\pi$, where $n = 1, 2, \dots$

Now suppose that a second distant quasi-monochromatic source is illuminated at an angle θ' from the bore sight of the interferometer. Assume that the sources are incoherent, meaning that the fields from the two sources are uncorrelated, and consequently, we do not have to consider interference effects between the sources.[†] Each source will therefore contribute its own fringe pattern in the interferometer, and the fringes of this second source will be offset from the fringes of the first because $\theta' \neq \theta$. The overall fringe pattern will simply be the sum of the fringes of each individual source. Thus, I will never reach a maximum of 4 times the power collected by one aperture, nor will it fall to a minimum of 0, so the fringe pattern from the pair of offset point sources is not as distinct as it would be if the pair of sources were collocated and together formed a point source. The “distinctness” of the fringes, referred to as the *visibility*, is defined as

$$V = \frac{I_{\max} - I_{\min}}{I_{\max} + I_{\min}}.$$

A point source is characterized by $V = 1$, and a pair of separated point sources (or any extended object, for that matter), is characterized by $V < 1$.

[†] A given point source is coherent with itself—this is what gives rise to the interferometer’s interference effects summarized in Equation 1. The subject of coherence will be covered in more depth in the next chapter.

The response of an amplitude interferometer can be used to do more than simply distinguish between point and extended sources—it can be used to measure the angular size of objects and can actually synthesize the image of an object. These concepts are developed in the following sections.

B. RESPONSE TO AN EXTENDED SOURCE

Consider a one-dimensional extended source of incoherent light. The flux of the extended source at the apertures is $F = F(\theta)$, and Equation 1 is valid for any given point-like element on the source:

$$I(\theta) d\theta = 2AF(\theta)[1 + \cos(kB\theta + \delta)] d\theta .$$

Because the source is incoherent, each $F(\theta)d\theta$ on the source is uncorrelated to any other, and the interferometer's response from the entire source is an integral over $I(\theta)d\theta$:

$$I = \int I(\theta) d\theta = 2A \int F(\theta) [1 + \cos(kB\theta + \delta)] d\theta .$$

Using the identity $\cos(A \pm B) = \cos A \cos B \mp \sin A \sin B$, we can rewrite the response as

$$I = 2A \left[\int F(\theta) d\theta + \cos \delta \int F(\theta) \cos kB\theta d\theta - \sin \delta \int F(\theta) \sin kB\theta d\theta \right] ,$$

or

$$I = 2A \left[\int F(\theta) d\theta + \text{Re} \left\{ e^{i\delta} \int F(\theta) e^{ikB\theta} d\theta \right\} \right] , \quad (2)$$

where $\text{Re}\{\}$ stands for the real part of the expression in parentheses. Equation 2 can be normalized to I_0 , the total power received by the two antennas:

$$I / I_0 = 1 + \text{Re} \left\{ e^{i\delta} \frac{\int F(\theta) e^{ikB\theta} d\theta}{\int F(\theta) d\theta} \right\} . \quad (3)$$

The *complex visibility* is defined as

$$\Gamma(B) \equiv \frac{\int F(\theta) e^{ikB\theta} d\theta}{\int F(\theta) d\theta} , \quad (4)$$

which is the normalized Fourier transform of the flux distribution $F(\theta)$. This definition can also be recast in terms of $|\Gamma(B)|$ and $\Phi(B)$, the modulus and the phase of the complex visibility:

$$\Gamma(B) = |\Gamma(B)| e^{i\Phi(B)} . \quad (5)$$

The modulus, or amplitude, which is bounded by 0 and 1, can be written as

$$|\Gamma(B)| = \frac{\left[\left(\int F(\theta) \cos kB\theta \, d\theta \right)^2 + \left(\int F(\theta) \sin kB\theta \, d\theta \right)^2 \right]^{\frac{1}{2}}}{\int F(\theta) \, d\theta} . \quad (6)$$

The phase gives the relationship between the real and complex parts of the transform.

Substituting Equations 4 and 5 into Equation 3, we get the normalized interferometer response to be

$$I/I_0 = 1 + \operatorname{Re} \left\{ e^{i\delta} |\Gamma(B)| e^{i\Phi(B)} \right\} ,$$

or simply

$$I/I_0 = 1 + |\Gamma(B)| \cos(\delta + \Phi(B)) . \quad (7)$$

The interferometer fringe response given in Equation 7 is pictured in Figure 2. The phase $\Phi(B)$ is the offset of the fringe modulation from $\delta = 0$ (which is the interferometer's optical path difference of 0). The quantity $|\Gamma(B)|$ is the amplitude of the fringe modulation. In fact, the amplitude can be written as

$$|\Gamma(B)| = \frac{I_{\max} - I_{\min}}{I_{\max} + I_{\min}} = V . \quad (8)$$

The modulus of the Fourier transform of the flux distribution is the visibility of the interferometer response as defined above.

C. THE AMPLITUDE INTERFEROMETER AS AN IMAGING DEVICE

Equation 4 shows that a source's flux distribution—or “brightness” distribution as it is called in astronomy—is the inverse Fourier transform of the complex visibility of a distant, incoherent source that subtends small angles. This relationship is known in optics as the van Cittert-Zernike theorem [1]. Since the complex visibility is measured by an interferometer, the interferometer's response can be inverted to obtain a brightness image of a source. Astronomers have coined this process *synthesis imaging* [2, 4].

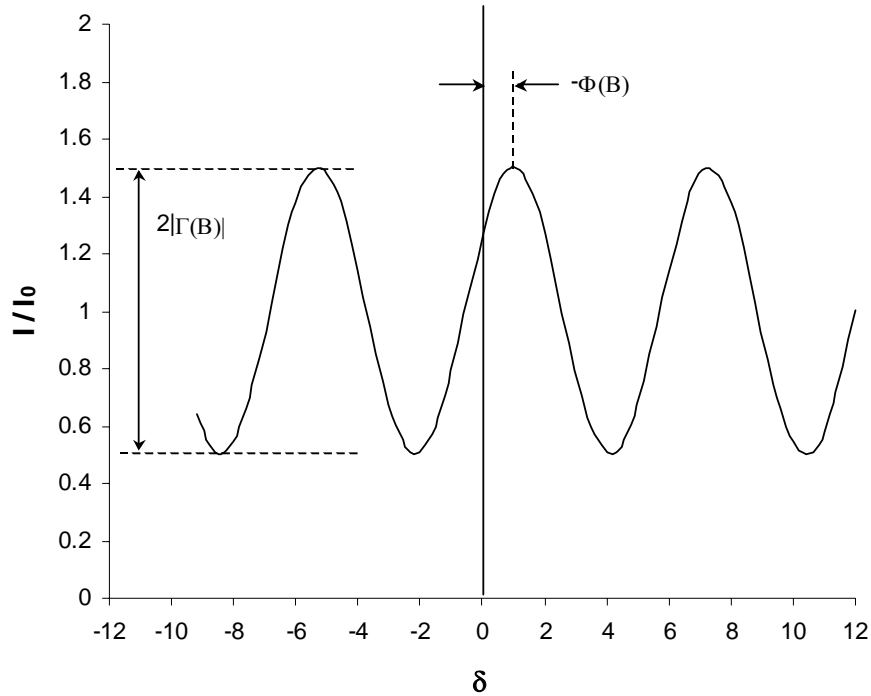


Figure 2. Response of an Amplitude Interferometer to an Extended Source

The difficulty level of synthesis imaging depends on the wavelength of the source radiation. This is primarily due to measuring the phase Φ , which is affected by atmospheric turbulence and instrumental instabilities. Although such measurements are possible in the radio frequency (RF) spectrum where wavelengths are macroscopic, it is quite a different story at optical wavelengths that are a fraction of a micron. The quantity V , on the other hand, is more readily measured at a variety of wavelengths from optical through RF wavelengths. One could imagine tracking and measuring the peaks and troughs in V in Figure 2, even as errors in the optical-path difference in the interferometer make the measurement of Φ impossible. At small wavelengths, however, even measurements of V are challenging.

So it is not surprising that synthesis imaging of the sort described above is generally the domain of radio astronomy, where antenna arrays, such as the National Radio Astronomy Observatory (NRAO) in Socorro, New Mexico, have been used to map cosmic radio emissions for decades.[‡] Synthesis imaging at optical wavelengths has only recently been undertaken [2]. (Note that synthesis imaging at optical wavelengths should

[‡] Background information on the NRAO facility and several extraordinary radio images are available through the NRAO website (<http://www.nrao.edu/>).

not be confused with standard optical imaging, where a single aperture and lens or lens group focuses light on an image plane.)

Although full synthesis imaging is exceedingly difficult at optical wavelengths, it is possible to measure V as discussed above. It has long been known that the angular size of an object can be extracted from V in a model-dependent manner when the object's shape is known. This will be shown in the next section. It is this technique that enabled Michelson and Pease and others to measure the diameter of stars a century ago.

D. VISIBILITY AND SOURCE MORPHOLOGY

1. Point Source

Consider a point source located at θ_0 :

$$F_{\text{point}}(\theta) = F_0 \delta(\theta - \theta_0) .$$

Replacing F_{point} in Equation 4 gives

$$\Gamma(B) = e^{ikB\theta_0} ,$$

which, when rewritten in the form of Equation 5, gives $|\Gamma(B)| = 1$ and $\Phi = kB\theta_0$. This simply gives the same result as in Equation 1. The visibility V , given by $|\Gamma(B)|$, is 1 for all values of B , so it is said that the source is unresolved by the interferometer (i.e., no physical extent is detected).

2. Binary System of Point Sources

Consider a binary system of point sources separated by angle α and centered at θ_0 :

$$F_{\text{binary}}(\theta) = F_0 \left[\delta(\theta - (\theta_0 + \alpha/2)) + \delta(\theta - (\theta_0 - \alpha/2)) \right] .$$

Replacing F_{binary} in Equation 4 gives

$$\begin{aligned} \Gamma(B) &= \frac{1}{2} \left(e^{ikB(\theta_0 + \alpha/2)} + e^{ikB(\theta_0 - \alpha/2)} \right) \\ &= e^{ikB\theta_0} \frac{1}{2} \left(e^{ikB\alpha/2} + e^{-ikB\alpha/2} \right) . \\ &= e^{ikB\theta_0} \cos\left(kB\alpha/2\right) . \end{aligned}$$

When rewritten in the form of Equation 5, we get the visibility $|\Gamma(B)| = \left| \cos\left(kB\alpha/2\right) \right|$ and the phase $\Phi = kB\theta_0$. The visibility of the binary system, shown as a solid line in Figure 3, reaches its first minimum at a baseline of $B = \lambda/2\alpha$. It is said that this source is resolved

by the interferometer because the visibility changes with baseline, unlike the single point source case where the visibility is 1 for all baselines.

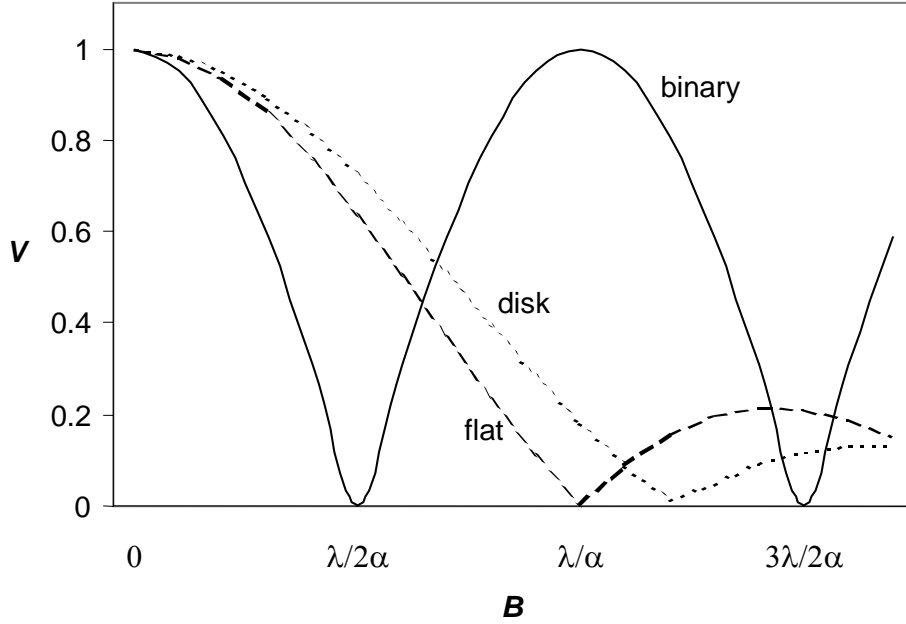


Figure 3. Visibility versus Baseline for (1) a Binary System of Point Sources Separated by Angle α , (2) a Flat Source that Subtends an Angle α , and (3) a Circular Source (Disk) that Subtends an Angle α

3. Flat Source Distribution

Consider a flat source distribution with an angular size α and centered at θ_0 :

$$F_{\text{flat}}(\theta) = \begin{cases} \frac{F_0}{\alpha} & \text{when } \theta_0 - \frac{\alpha}{2} < \theta < \theta_0 + \frac{\alpha}{2} \\ 0 & \text{otherwise} \end{cases} .$$

Replacing F_{flat} in Equation 4 gives

$$\begin{aligned} \Gamma(B) &= \frac{1}{ikB\alpha} \left(e^{ikB(\theta_0 + \alpha/2)} - e^{ikB(\theta_0 - \alpha/2)} \right) \\ &= e^{ikB\theta_0} \frac{1}{ikB\alpha} \left(e^{ikB\alpha/2} - e^{-ikB\alpha/2} \right) . \\ &= e^{ikB\theta_0} \frac{\sin(kB\alpha/2)}{(kB\alpha/2)} \end{aligned}$$

When rewritten in the form of Equation 5, we get the visibility $|\Gamma(B)| = \left| \frac{\sin(kB\alpha/2)}{(kB\alpha/2)} \right|$ and the phase $\Phi = kB\theta_0$. The visibility of the flat system, shown as a dashed line in

Figure 3, reaches its first minimum at a baseline of $B = \lambda/\alpha$. Again, this source is resolved by the interferometer because the visibility changes with baseline.

4. Circular Source Distribution

Consider a uniformly bright circular source distribution (a disk) with an angular size α , centered on the interferometer's bore sight ($\theta_0 = 0$), as pictured in Figure 4. The denominator of the visibility integral in Equation 4, which integrates $F_{\text{disk}}(\theta)$ over the extent of the source, is simply

$$\int F(\theta)d\theta = \int_{-\alpha/2}^{\alpha/2} h(\theta)d\theta \quad ,$$

where h is pictured in the figure. It is possible to change variables from θ to x as shown in the figure so that $F(\theta) \rightarrow F_{\text{disk}}(x) = \alpha \cos x$, $\theta = (\alpha/2) \sin x$, and $d\theta = (\alpha/2) \cos x dx$. The limits on the integral also change: $\theta = \pm \alpha/2 \rightarrow x = \pm \pi/2$. Thus,

$$\int F(\theta)d\theta = \int_{-\pi/2}^{\pi/2} \frac{\alpha^2}{2} \cos^2 x dx = \frac{\alpha^2 \pi}{4} \quad . \quad (9)$$

The numerator of Equation 4 is then

$$\int F(\theta)e^{ikB\theta}d\theta = \int_{-\pi/2}^{\pi/2} \frac{\alpha^2}{2} \cos^2 x e^{ikB\alpha/2} dx = \frac{\pi\alpha}{kB} J_1(kB\alpha/2) \quad . \quad (10)$$

Combining Equations (9) and (10) gives

$$\Gamma(B) = 2 \frac{J_1(kB\alpha/2)}{(kB\alpha/2)} \quad .$$

When rewritten in the form of Equation 5, we get the visibility for a uniformly bright disk as $|\Gamma(B)| = \left| 2 \frac{J_1(kB\alpha/2)}{(kB\alpha/2)} \right|$, which is shown as a dotted line in Figure 3. The disk's visibility reaches its first minimum at a baseline of $B = 1.22\lambda/\alpha$. Again, this source is resolved by the interferometer because the visibility changes with baseline.

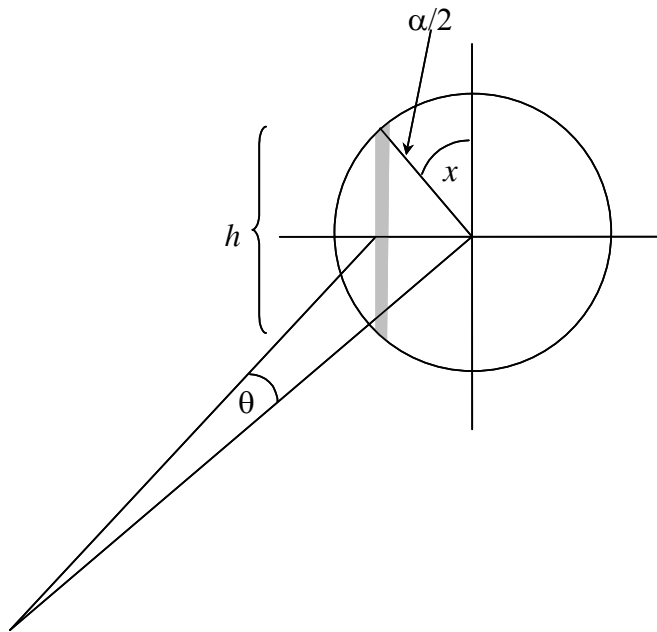


Figure 4. Geometry for a Circular (Disk-Shaped) Source that Subtends an Angle α

III. INTENSITY INTERFEROMETRY

As discussed above, measurements with an amplitude interferometer can be difficult. R. Hanbury-Brown and R.Q. Twiss made the remarkable realization that the modulus of the complex visibility of a source can be measured by correlating the *intensities* of two detectors separated in space [3]. As will be seen, there are important advantages, as well as some drawbacks, to using this approach.

Figure 5 shows a schematic of an intensity interferometer. The outputs of two square-law detectors[§] are fed into low-pass filters and then correlated. The correlation function computed at the final stage is effectively

$$C(\tau) = \frac{1}{T} \int_0^T I_a(t) I_b(t + \tau) dt \quad , \quad (11)$$

where I_a and I_b are the filtered intensities, and the maximum of the correlation is at $\tau = 0$, which corresponds to the optical path difference of 0. The correlation is simply the time average of I_a and I_b over time T .

Before deriving the relationship between the correlation of intensity fluctuations and the visibility of a source, we consider a simple model for an incoherent source, which is important to the derivation of the Hanbury Brown and Twiss (HBT) effect.

A. MODEL FOR AN INCOHERENT (THERMAL) SOURCE

The response of an amplitude interferometer is typically derived by considering a monochromatic, incoherent source. A monochromatic source is by definition coherent, however, so the incoherence in the derivation of the amplitude interferometer is included in an ad hoc manner by ignoring the correlations between different parts of the source. A source with a finite bandwidth is needed to understand the HBT effect.

A wave can be defined as coherent if it is possible to predict its phase over arbitrarily long times. If it is only possible to predict a wave's phase over time $\sim \tau_c$, it is said that the wave is partially coherent with a coherence time τ_c .

[§] A square-law detector is one whose output is proportional to the intensity of the input field.

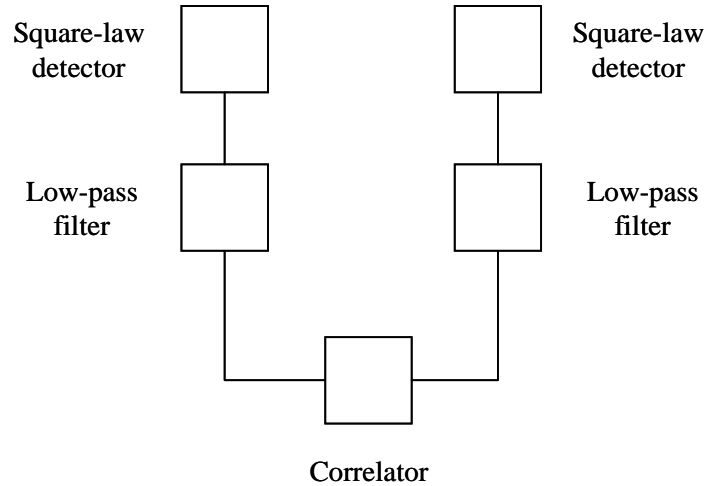


Figure 5. Elements of an Intensity Interferometer

Finite coherence time implies finite bandwidth. To see this, consider a constant-amplitude wave train, $F(t)$, that has phase stability for time periods exactly τ_c . The spectral density of this wave train is based on its basic part, namely a harmonic wave with frequency ω_0 and amplitude f_0 :

$$F(t) = f_0 e^{-i\omega_0 t} \quad |t| \leq \frac{\tau_c}{2}$$

$$F(t) = 0 \quad |t| > \frac{\tau_c}{2}.$$

The spectral density, $f(\omega)$, of $F(t)$ is given by its Fourier transform:

$$f(\omega) = \int e^{i\omega t} F(t) dt = \int_{-\tau_c/2}^{\tau_c/2} f_0 e^{i(\omega - \omega_0)t} dt$$

$$= f_0 \tau_c \left[\frac{\sin(\omega - \omega_0)\tau_c / 2}{(\omega - \omega_0)\tau_c / 2} \right].$$

The intensity distribution is then $f(\omega)^2$, which has its first zero when the argument of sine is equal to π , corresponding to the width

$$(\omega - \omega_0)\tau_c / 2 = \pi$$

or $\Delta\nu = 1/\tau_c$.

Thus, the bandwidth is related to the finite coherence time.

For the purposes of this study, an incoherent wave train can be constructed by using a monochromatic wave with random phase jumps, uniformly distributed between 0

and 2π , that occur on average every τ_c .[√] The actual distribution in time for the phase jumps is not important; a flat or Gaussian distribution with a mean of τ_c , or even a phase change every τ_c , would work to develop the HBT concept.

B. DERIVATION OF THE HBT EFFECT

Figure 6 is a schematic diagram of two identical detectors, a and b , viewing a source consisting of many points such as m and n . The detectors, which measure intensity, are read out as pictured in Figure 5. The field due to point m at detector a is given by

$$A_m^a = A_m \cos(kR_m^a - \omega t + \phi_m) \quad ,$$

where the phase ϕ_m is a time-dependent quantity ($\phi_m = \phi_m(t)$) that changes with a period that is, on average, equal to the source's coherence time τ_c . The phase changes are randomly distributed between 0 and 2π .

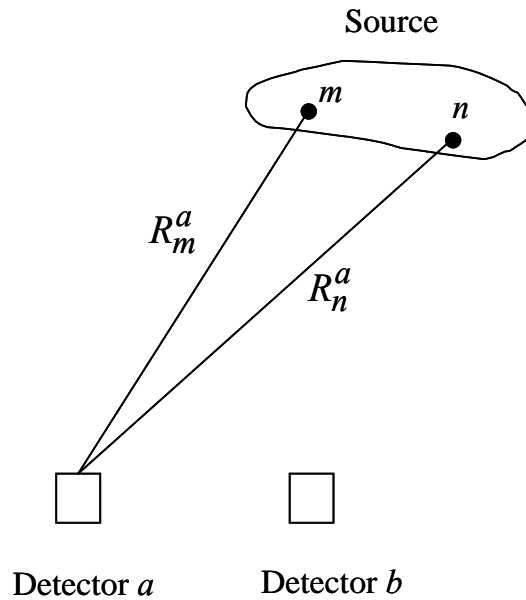


Figure 6. Schematic Diagram of an Intensity Interferometer Viewing a Source

The field from the whole source at a is then

[√] This construct, though an oversimplification, does access an important characteristic of a thermal source, namely that the phase of an emitting atom is interrupted because of atomic collisions. Although there are other effects in thermal emissions, such as the damping of wave trains as atoms lose energy during emission and the Doppler-broadening of lines [1], these are not necessary to understanding HBT.

$$A^a = \sum_m A_m \cos(kR_m^a - \omega t + \phi_m) \quad ,$$

and the intensity, I_a , is

$$\begin{aligned} I_a &= (A^a)^2 = \left[\sum_m A_m \cos(kR_m^a - \omega t + \phi_m) \right] \left[\sum_n A_n \cos(kR_n^a - \omega t + \phi_n) \right] \\ &= \frac{1}{2} \sum_m \sum_n A_m A_n \left[\cos(k(R_m^a - R_n^a) + \phi_m - \phi_n) + \cos(k(R_m^a + R_n^a) - 2\omega t + \phi_m + \phi_n) \right] \end{aligned} \quad ,$$

where we have used the identity $\cos x \cos y = \frac{1}{2}[\cos(x+y) + \cos(x-y)]$. Assuming the detector's output is low-pass filtered, we are left with

$$\begin{aligned} I_a &= \frac{1}{2} \sum_m \sum_n A_m A_n \cos(k(R_m^a - R_n^a) + \phi_m - \phi_n) \\ &= \frac{1}{2} \sum_m A_m^2 + \frac{1}{2} \sum_{m \neq n} A_m A_n \cos(k(R_m^a - R_n^a) + \phi_m - \phi_n) \end{aligned} \quad . \quad (12)$$

We are interested in computing Equation 11, which is the time average of the intensities of detectors a and b . The time average is much longer than the coherence time of the source. If we denote the time average of the intensities at $\tau = 0$ with angle brackets, we have

$$\begin{aligned} \langle I_a I_b \rangle &= \frac{1}{4} \left\langle \sum_m \sum_{m'} A_m^2 A_{m'}^2 + \text{terms linear in cosine} \right. \\ &\quad \left. + \sum_{m \neq n} \sum_{m' \neq n'} A_m A_n A_{m'} A_{n'} \cos[k(R_m^a - R_n^a) + \phi_m - \phi_n] \right. \\ &\quad \left. \cdot \cos[k(R_{m'}^b - R_{n'}^b) + \phi_{m'} - \phi_{n'}] \right\rangle \quad . \quad (13) \end{aligned}$$

The terms linear in cosine will time average to 0 because the time average is much longer than the coherence time, hence jumps in phase (ϕ) will cause the cosine to average to 0.

The last term in Equation 13 can be rewritten as:

$$\begin{aligned} &\left\langle \sum_{m \neq n} \sum_{m' \neq n'} A_m A_n A_{m'} A_{n'} \cos[k(R_m^a - R_n^a) + \phi_m - \phi_n] \cos[k(R_{m'}^b - R_{n'}^b) + \phi_{m'} - \phi_{n'}] \right\rangle \\ &= \left\langle \sum_{m \neq n} \sum_{m' \neq n'} A_m A_n A_{m'} A_{n'} \left\{ \frac{1}{2} \cos[k(R_m^a - R_n^a - R_{m'}^b + R_{n'}^b) + \phi_m - \phi_n - \phi_{m'} + \phi_{n'}] \right. \right. \\ &\quad \left. \left. + \frac{1}{2} \cos[k(R_m^a - R_n^a + R_{m'}^b - R_{n'}^b) + \phi_m - \phi_n + \phi_{m'} - \phi_{n'}] \right\} \right\rangle \quad . \quad (14) \end{aligned}$$

The first term on the right-hand side of Equation 14 survives the time average only if $m = m'$ and $n = n'$, or else the phases (ϕ terms) remain, which, over time, cause the cosine to

average to 0. Similarly, the second term survives only if $m = n'$ and $n = m'$. Thus Equation 14 reduces to

$$\begin{aligned} & \left\langle \sum_{m \neq n, m' \neq n'} \sum A_m A_n A_{m'} A_{n'} \cos[k(R_m^a - R_n^a) + \phi_m - \phi_n] \cos[k(R_{m'}^b - R_{n'}^b) + \phi_{m'} - \phi_{n'}] \right\rangle \\ & = \sum_{m \neq n} A_m^2 A_n^2 \cos[k(R_m^a - R_m^b - R_n^a + R_n^b)] \end{aligned}$$

Substituting this result into Equation 13 gives

$$\langle I_a I_b \rangle = \left(\frac{1}{2} \sum_m A_m^2 \right)^2 + \frac{1}{4} \sum_{m \neq n} A_m^2 A_n^2 \cos[k(R_m^a - R_m^b - R_n^a + R_n^b)] \quad (15)$$

The time-averaged power from one detector, as given by Equation 12, is simply

$$\langle I_a \rangle = \frac{1}{2} \sum_m A_m^2, \quad (16)$$

because the leftover phases cause the second term of Equation 12 to time average to 0. Both detectors, a and b , will measure the same time-averaged power as given in Equation 16, which can be called simply $\langle I \rangle$. We can then normalize Equation 15:

$$\frac{\langle I_a I_b \rangle}{\langle I \rangle^2} = 1 + \frac{\sum_{m \neq n} A_m^2 A_n^2 \cos[k(R_m^a - R_m^b - R_n^a + R_n^b)]}{\left(\sum_m A_m^2 \right)^2}.$$

Inspection of Figure 7 shows that $R_m^a - R_m^b = B\theta_m$, thus

$$\frac{\langle I_a I_b \rangle}{\langle I \rangle^2} = 1 + \frac{\sum_{m \neq n} A_m^2 A_n^2 \cos[kB(\theta_m - \theta_n)]}{\left(\sum_m A_m^2 \right)^2}.$$

Rewriting the limits on the summation gives

$$\frac{\langle I_a I_b \rangle}{\langle I \rangle^2} = 1 - \frac{\sum_m A_m^4}{\left(\sum_m A_m^2 \right)^2} + \frac{\sum_{m,n} A_m^2 A_n^2 \cos[kB(\theta_m - \theta_n)]}{\left(\sum_m A_m^2 \right)^2}. \quad (17)$$

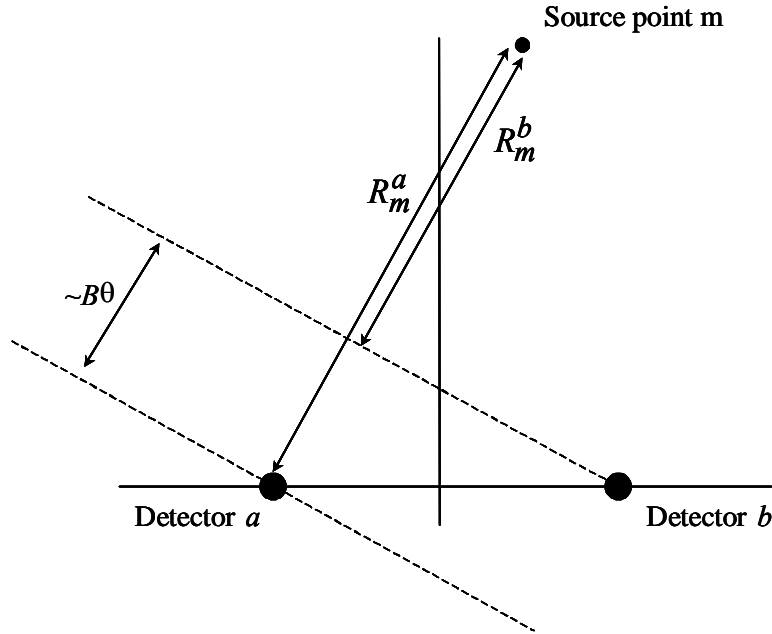


Figure 7. Path Length Difference for Radiation Arriving at Detectors *a* and *b*. *B* is the baseline of the two detectors and θ is the angle of source point *m* from the interferometer's bore sight.

Consider the second term on the right-hand side of Equation 17. Assume that the source to be imaged consists of N equal-strength point sources and that the interferometer is capable of resolving the points within the source (i.e., λ/B is small enough to do this). The second term in Equation 17 then reduces to

$$\frac{\sum_m A_m^4}{\left(\sum_m A_m^2\right)^2} \rightarrow \frac{1}{N},$$

which vanishes in the limit of a source built of many points. Another way to view this is that if the interferometer resolution is small compared to the angular size of the source, and if the changes in brightness are not too dramatic across the source, then this term can be ignored. This term cannot be ignored if the source to be imaged is made of a small number of points, or if it is made of many points but with a few that are much brighter than the rest. Nevertheless, for many interesting cases—where complex sources are viewed by interferometers with adequate resolution—this term can be ignored.

The third term in Equation 17 can be rewritten using the definition for $\langle I \rangle$ and the identity $\cos(A - B) = \cos A \cos B + \sin A \sin B$:

$$\begin{aligned} \frac{\sum_{m,n} A_m^2 A_n^2 \cos[kB(\theta_m - \theta_n)]}{\left(\sum_m A_m^2\right)^2} &= \frac{1}{\langle I \rangle^2} \sum_{m,n} A_m^2 A_n^2 (\cos kB\theta_m \cos kB\theta_n + \sin kB\theta_m \sin kB\theta_n) \\ &= \frac{1}{\langle I \rangle^2} \left[\left(\sum_m A_m^2 \cos kB\theta_m\right)^2 + \left(\sum_m A_m^2 \sin kB\theta_m\right)^2 \right] \end{aligned}$$

Noting that A_m^2 is just the intensity (or brightness) F_m of the point, and converting sums into integrals by replacing $F_m \rightarrow F(\theta)d\theta$, the intensity correlation in Equation 17 can be rewritten as

$$\frac{\langle I_a I_b \rangle}{\langle I \rangle^2} = 1 + \frac{1}{\langle I \rangle^2} \left[\left(\int F(\theta) \cos kb\theta d\theta\right)^2 + \left(\int F(\theta) \sin kb\theta d\theta\right)^2 \right].$$

A comparison of this result to Equation 6 shows that the intensity correlation is given by

$$\frac{\langle I_a I_b \rangle}{\langle I \rangle^2} = 1 + |\Gamma(B)|^2. \quad (18)$$

The intensity correlation measures the modulus (but not the phase) of the Fourier transform of the source distribution.

C. ADVANTAGES AND LIMITATIONS OF THE HBT EFFECT

HBT cannot be used to fully image a complex source because it measures only the modulus (and not the phase) of the complex visibility. Knowledge of the phase is necessary to invert the complex visibility and obtain the source's brightness distribution. HBT can be used to measure, in a model-dependent fashion, the size of objects whose shape is known. An obvious application of this is the measurement of the angular size of stars. It can also be used to obtain the approximate size of an object whose shape is not known. This can be seen by examining Figure 3, which shows the modulus of the complex visibility for different source shapes. Although the specific source shape will determine the precise baseline at which the magnitude of the visibility vanishes, HBT measurements can give an approximate measurement of the size of the overall source—the first minimum in visibility for a binary, flat, or circular source is within a factor of 2.5 of one another as shown in the figure.

Within the context of measuring the modulus of the complex visibility, there are advantages and disadvantages of using HBT instead of amplitude interferometry. One

advantage is that HBT is less sensitive to atmospheric turbulence and device instabilities. In amplitude interferometry, the phase of the incident radiation after having taken separate paths through the medium is measured at two separate detectors. A fluctuating medium or device instabilities that induce path length errors of order a wavelength would seriously affect the accuracy of the measurement. The HBT interferometer need not preserve the stability at the level of the incident radiation wavelength. Instead, stability only on the level of the coherence time is needed, hence the interferometer is less sensitive to atmospheric effects and device instabilities. HBT's disadvantage is that it has diminished sensitivity for dim sources because the signal-to-noise ratio at the HBT correlator goes as $(P_S/P_N)^2$, where P_S and P_N are the signal and noise power at detectors. In an amplitude interferometer, the overall signal-to-noise ratio goes as P_S/P_N .

D. EXTENSION OF HBT

HBT measurements cannot image a complicated source because they do not provide the phase of the Fourier transform of a source's brightness distribution; however, methods have been developed to extract the phase information in intensity correlations. Gamo proposed the superposition of a coherent beam on the measurement of an unknown source [5].# In another approach, Mehta proposed that a source with known but finite coherence be used to extract the phase data [6]. This approach was demonstrated in the lab [7]. Although resources preclude developing these ideas in detail here, we offer a brief summary that follows [6]. The visibility of an unknown source is measured to be V using standard HBT measurements. A reference source with known visibility and phase, V_0 and Φ_0 , is superimposed on the unknown source, and the visibility of the combined source, \tilde{V} , is also measured using standard HBT techniques. The visibility of the combined source is given by $\tilde{V}^2 = V^2 + V_0^2 + 2VV_0 \cos(\Phi - \Phi_0)$, where Φ is the phase of the unknown source. Since all of the quantities except Φ in the expression for \tilde{V}^2 are either known or measured, $\Phi - \Phi_0$ can be solved to within a factor of -1 . The sign ambiguity results in an inverted and uninverted image [7]. This process is analogous to holography.**

Gamo further proposed extracting the lost phase information by using triple correlations, or correlations of three detector elements. See [5] for details.

** T. D. Beard, private communication.

IV. SUMMARY

An amplitude interferometer measures the modulus and phase of the Fourier transform of the brightness distribution of an incoherent source, thus the response of the amplitude interferometer can be inverted to obtain an image of the source. This imaging process is dependent on the ability of the device to accurately track the phase of the incident radiation field. A traditional intensity interferometer measures only the modulus of the Fourier transform of a source's brightness distribution. It cannot fully reconstruct a complex source because the device does not measure phase information of the Fourier transform. This type of device is nevertheless able to approximate a source's size, and, in the case where the source's shape is known, a precise size estimate can be extracted in a model-dependent manner.

Extensions to the intensity interferometer enable this type of device to fully image a source. These approaches involve the superposition of a known source onto the device or processing triple correlations among interferometer elements (as opposed to double correlations).

It is appropriate to use an amplitude interferometer when the phase of radiation can be measured. A source can be fully imaged with this type of interferometer, and the signal-to noise ratio for dim sources is higher in this device than in intensity interferometers. If tracking the phase of radiation is difficult, as when dealing with small wavelengths or atmospheric or device instabilities that cause phase measurement errors, then intensity interferometers are appropriate. Although the signal-to-noise ratio of an intensity interferometer suffers when the source is dim, it is more robust in a turbulent medium. Traditional intensity interferometers are limited as imaging devices; however, extensions to the intensity interferometer allow for sources to be fully imaged.

REFERENCES

- [1] M. Born and E. Wolf, *Principles of Optics* (Oxford: Pergamon Press, 1964).
- [2] A.F. Boden, "Elementary Theory of Interferometry," in *Principles of Long Baseline Stellar Interferometry*, course notes from the 1999 Michelson Summer School, edited by P. R. Lawson (Jet Propulsion Laboratory Publication 00-009 07/00), Chapter 2. Available online at <http://sim.jpl.nasa.gov/michelson/iss.html>.
- [3] R. Hanbury Brown and R. Q. Twiss, "A New Type of Interferometer for Use in Radio Astronomy," *Philosophical Magazine* **45**, 663 (1954).
- [4] A.R. Thompson, J.M. Moran, and G.W. Swenson, *Interferometry and Synthesis in Radio Astronomy* (New York: John Wiley & Sons, 1986).
- [5] H. Gamo, "Phase Determination of Coherence Functions by the Intensity Interferometer," *Electromagnetic Theory and Antennas*, edited by E.C. Jordan (Oxford: Pergamon Press, 1963), p. 801.
- [6] C.L. Mehta, "New Approach to the Phase Problem in Optical Coherence Theory," *Journal of the Optical Society of America* **58**, 1233 (1968).
- [7] T.D. Beard, "Imaging by Correlation of Intensity Fluctuations," *Applied Physics Letters* **15**, 227 (1969).

REPORT DOCUMENTATION PAGE*Form Approved*
OMB No. 0704-0188

Public reporting burden for this collection of information is estimated to average 1 hour per response, including the time for reviewing instructions, searching existing data sources, gathering and maintaining the data needed, and completing and reviewing this collection of information. Send comments regarding this burden estimate or any other aspect of this collection of information, including suggestions for reducing this burden to Department of Defense, Washington Headquarters Services, Directorate for Information Operations and Reports (0704-0188), 1215 Jefferson Davis Highway, Suite 1204, Arlington, VA 22202-4302. Respondents should be aware that notwithstanding any other provision of law, no person shall be subject to any penalty for failing to comply with a collection of information if it does not display a currently valid OMB control number. **PLEASE DO NOT RETURN YOUR FORM TO THE ABOVE ADDRESS.**

1. REPORT DATE June 2004		2. REPORT TYPE Final		3. DATES COVERED (From-To) July 2003 – May 2004	
4. TITLE AND SUBTITLE Imaging with Amplitude and Intensity Interferometers				5a. CONTRACT NUMBER DAS W01 98 C 0067/DASW01-04-C-0003	
				5b. GRANT NUMBER	
				5c. PROGRAM ELEMENT NUMBER	
6. AUTHOR(S) Frank Rotondo				5d. PROJECT NUMBER	
				5e. TASK NUMBER IDA Central Research Project C2064/C2084	
				5f. WORK UNIT NUMBER	
7. PERFORMING ORGANIZATION NAME(S) AND ADDRESS(ES) Institute for Defense Analyses 4850 Mark Center Drive Alexandria, VA 22311-1882				8. PERFORMING ORGANIZATION REPORT NUMBER IDA Document D-2999	
9. SPONSORING / MONITORING AGENCY NAME(S) AND ADDRESS(ES) Institute for Defense Analyses 4850 Mark Center Drive Alexandria, VA 22311-1882				10. SPONSOR/MONITOR'S ACRONYM(S)	
				11. SPONSOR/MONITOR'S REPORT NUMBER(S)	
12. DISTRIBUTION / AVAILABILITY STATEMENT Approved for public release; distribution unlimited.					
13. SUPPLEMENTARY NOTES					
14. ABSTRACT Amplitude and intensity interferometers are powerful imaging devices. An amplitude interferometer measures the modulus and phase of the Fourier transform of the brightness distribution of an incoherent source, thus the response of the amplitude interferometer can be inverted to obtain an image of the source. A traditional intensity interferometer measures only the modulus of the Fourier transform of a source's brightness distribution. It cannot fully reconstruct a complex source because the device does not measure phase information of the Fourier transform. This type of device is nevertheless able to approximate a source's size, and, in the case where the source's shape is known, a precise size estimate can be extracted in a model-dependent manner. Extensions to the traditional intensity interferometer, however, enable it to fully image a source. This document derives the responses of amplitude and intensity interferometers, and discusses the advantages and limitations of each type of device.					
15. SUBJECT TERMS Imaging, interferometer, interferometry					
16. SECURITY CLASSIFICATION OF:			17. LIMITATION OF ABSTRACT SAR	18. NUMBER OF PAGES 28	19a. NAME OF RESPONSIBLE PERSON Frank Rotondo
a. REPORT Uncl.	b. ABSTRACT Uncl.	c. THIS PAGE Uncl.			19b. TELEPHONE NUMBER (include area code) 703-845-6768

